arXiv:1508.06004v2 [cond-mat.mes-hall] 7 Nov 2015

Photo-Conductivity Response at Cyclotron-Resonance Harmonics in a Non-Degenerate 2D Electron Gas on Liquid Helium

R. Yamashiro,[1] L. V. Abdurakhimov,[1] A. O. Badrutdinov,[1] Yu. P. Monarkha,[2] and D. Konstantinov[1, *]

[1] *Okinawa Institute of Science and Technology, Tancha 1919-1, Okinawa 904-0495, Japan*

[2] *Institute for Low Temperature Physics and Engineering, 47 Lenin Avenue, 61103, Kharkov, Ukraine*

(Dated: November 10, 2015)

We report the first observation of an oscillatory photo-conductivity response at the cyclotron-resonance harmonics in a non-degenerate 2D electron system formed on the free surface of liquid helium. The dc conductivity oscillations are detected for electrons occupying the ground surface subband. Their period is governed by the ratio of the microwave frequency to the cyclotron frequency. Theoretical analysis of the photo-response in a strongly interacting electron system indicates that the observation can be explained by an oscillatory correction to the electron distribution function that appears for a large inelastic relaxation time because of photon-assisted scattering.

PACS numbers: 73.20.-r, 73.21.-b, 73.63.Hs, 78.20.Ls, 78.56.-a

Two-dimensional (2D) electrons in a perpendicular magnetic field B populate equidistant Landau levels, and, under certain conditions, can resonantly interact with the microwave (MW) electric field of frequency ω. Selection rules allow direct photon-induced transitions only between adjacent states ($n' - n = \pm 1$), as in the cyclotron resonance (CR) at $\omega_c \to \omega$ ($\omega_c = eB/M_e c$ is the cyclotron frequency). However, photon-assisted scattering of electrons from system disorder can lead to a remarkable photo-response in electron transport at CR harmonics ($m\omega_c = \omega$), where $m = 2, 3, ...$ is an integer. Magneto-oscillations in the dc resistivity and conductivity of a 2D electron gas discovered in high-mobility GaAs/AlGaAs heterostructures [1–4] represent an outstanding example of such a photo-response. An important feature of these oscillations is that they are governed by the ratio ω/ω_c. In the vicinity of $\omega/\omega_c = m$ both the resistivity and conductivity curves have asymmetrical shape with minima near $\omega/\omega_c = m + 1/4$. At low temperatures and strong enough power, resistivity minima evolve into zero-resistance states (ZRS).

Various theoretical mechanisms have been proposed to explain these microwave-induced resistance oscillations (MIRO) and ZRS (for a review see [5]), but the subject is still under debate. For two most elaborated mechanisms of MIRO proposed for semiconductor systems ("displacement" [6, 7] and "inelastic" [8, 9]), electron gas degeneracy is not a crucial point. Therefore, the same kind of magneto-oscillations governed by ω/ω_c potentially can appear in a nondegenerate 2D system of surface electrons (SEs) on liquid helium. A different type of microwave-induced magnetoconductivity oscillations is observed in this system [10, 11] when the inter-subband frequency $(\Delta_2 - \Delta_1)/\hbar = \omega_{2,1}$ matches ω (here Δ_1 and Δ_2 are the energies of the ground and first excited surface subbands, respectively). This phenomenon was explained [12–14] by nonequilibrium population of the second surface subband which triggers quasi-elastic inter-subband scattering against or along the driving force, depending on the relation between $\Delta_2 - \Delta_1$ and the Landau excitation energy $m\hbar\omega_c$. It was found that oscillations vanished if ω was substantially different from $\omega_{2,1}$, which means that they are actually governed by the ratio $\omega_{2,1}/\omega_c$.

The displacement mechanism of MIRO is based on the effect of the strong MW field on in-plane electron scattering. A displacement of the electron orbit center $X' - X$ which follows from energy conservation for photon-assisted scattering by impurities depends strongly on the relation between $\hbar\omega$ and $\hbar\omega_c$. In the inelastic mechanism, MIRO is caused by an oscillatory correction to the electron distribution function which appears because of photon-assisted scattering to high Landau levels ($n' - n = m$) and a large inelastic relaxation time. Theoretical analysis [15] indicates that for electrons on liquid helium, the photon-assisted scattering, which is important for both mechanisms, is weaker than it is in GaAs/AlGaAs by the factor $M_e^*/M_e \sim 0.06$, where M_e^* is the effective mass of electrons in GaAs/AlGaAs. Therefore, observation of MIRO in a single subband of SEs on liquid helium requires significantly higher MW power. This explains why MIRO, governed by the ratio ω/ω_c, was not detected previously for electrons on liquid helium.

In this Letter, we report the first observation of ω/ω_c-periodic dc-magnetoconductivity oscillations induced by the MW in the ground subband of a nondegenerate 2D electron system on the surface of liquid ^{4}He. In our experiment, the MW electric field polarized in the 2D plane is significantly enhanced by employing a high Q-factor resonator. This allows us to reach the necessary MW field sufficient to compensate for the reduction in photon-assisted scattering of SEs caused by the free-electron mass M_e and to produce a strong electron photo-response at CR harmonics. Results obtained are compared with outcomes of the displacement and inelastic models of MIRO applied to the nondegenerate strongly interacting 2D electron system on liquid helium.

The sketch of our experimental cell is shown in Fig. 1. The important feature of our experimental method

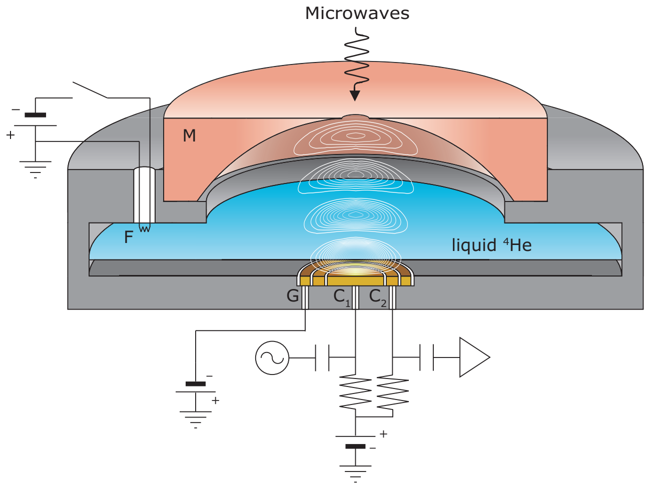

FIG. 1: (color online) Sketch of the experimental cell. White lines show calculated electric field contours for TEM$_{003}$ mode. The pool of 2D electrons (not shown) is formed on the liquid surface above electrodes C$_1$ (central) and C$_2$ (middle). Further details are provided in the text.

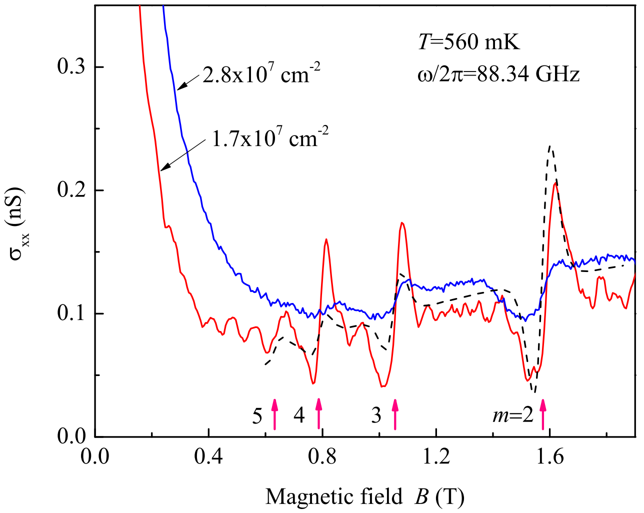

FIG. 2: (color online) σ_{xx} versus B for surface electrons in the Fabry-Perot resonator. Data are taken at a fixed input MW power, and for two electron densities $n_s = 2.8 \times 10^7$ (blue) and 1.7×10^7 cm^{-2} (red). Arrows indicate positions of $m = \text{round}\,(\omega/\omega_c)$. Theoretical results obtained using the inelastic model for the lowest n_s are shown by the dashed line (black).

is a semi-confocal Fabry-Perot resonator operating in TEM$_{003}$ mode [16]. The resonator is formed by two coaxial mirrors. The top spherical (radius of curvature 9 mm) mirror M is made of high purity copper. The bottom flat circular mirror (diameter 5.2 mm) is made of gold vaporized onto a sapphire substrate and is divided into three concentric electrodes C$_1$, C$_2$ and G by two gaps (width 0.01 mm) 1.5 and 2.13 mm from the center. Microwaves are produced by a broad-band (75-110 GHz) source at room temperature, passed through an attenuator and a low-pass filter (40 dB rejection above 139 GHz), and guided into the cryostat. There, microwaves are coupled from the waveguide to the resonator through an aperture (diameter 1.3 mm) at the center of the mirror M. Below 1 K, TEM$_{003}$ mode has a frequency of 88.52 GHz and the quality factor $Q \approx 900$. There are three nodes and four antinodes of the electric field E_{MW} between the mirrors. Calculated contours of E_{MW} are plotted in Fig. 1. The fourth antinode, where E_{MW} has the global maximum value, is located about 1.0 mm from the flat mirror. The waist of the Gaussian beam at this antinode is about 4.0 mm.

The ^{4}He gas is condensed into the cell and the liquid level is set between the mirrors. During condensation, the resonant frequency of the Fabry-Perot cavity, which is monitored by measuring the MW signal reflected from the cavity, shifts due to a change in the dielectric constant of the media filling the cavity. This allows us to set the liquid level at the fourth antinode of E_{MW}. Electrons are produced by briefly heating a tungsten filament F, while a positive bias is applied to electrodes C$_1$ and C$_2$. The 2D electrons form a circular pool on the liquid surface above the biased electrodes, and the areal density can be approximately determined from the condition of complete screening of the static electric field above the charged surface [11]. After charging, a negative bias is applied to the guard electrode G to prevent charge leakage into and from the pool. The diagonal dc conductivity σ_{xx} of the 2D electron liquid is measured by a standard capacitive coupling method [17] using electrodes C$_1$ and C$_2$ as a Corbino disk. Conductivity values are extracted from experimental data using a numerical procedure similar to that described previously [11].

At $T < 0.7$ K SEs are predominantly scattered by surface excitations of liquid helium (ripplons). Ripplons represent a sort of 2D phonons with the capillary wave spectrum $\omega_{r,q} = \sqrt{\alpha/\rho}q^{3/2}$ (here α and ρ are the surface tension and mass density of liquid helium respectively). The electron-ripplon scattering is similar to usual electron-phonon scattering in solids; it is described by the parameter $U_q = V_{r,q} Q_q N_q^{1/2}$, where $V_{r,q}$ is the electron-ripplon coupling [18], $Q_q^2 = \hbar q/2\rho\omega_{r,q}$, and N_q is the ripplon distribution function. The momentum relaxation rate of SEs is determined by quasi-elastic, one-ripplon scattering with long wavelength ripplons $q \sim 1/l_B$, which yields $N_q \simeq T/\hbar\omega_{r,q}$ and $\hbar\omega_{r,q} \ll \Gamma_n$, where $l_B^2 = \hbar c/eB$, and Γ_n is the Landau level broadening. Thus, under usual conditions $\hbar\omega_c \gg T$ and $\Gamma_n \ll T$, nearly all electrons occupy the lowest Landau level, which distinguishes SEs on liquid helium from electrons in GaAs/AlGaAs.

Figure 2 shows σ_{xx} versus B for two values of the electron density n_s. Data are taken at $T = 0.56$ K and a fixed power of 2.95 mW measured at the output of the MW source. This corresponds to the power incident on the resonator $P_{in} \approx 100\ \mu$W. Higher source output power caused overheating of the refrigerator; therefore it was avoided. Microwave frequency was adjusted to excite resonant TEM$_{003}$ mode. According to our estimations, almost all incident microwave power at resonance is dissipated inside the cavity. For $P_{in} = 100\ \mu$W, we obtain the energy stored in the resonator (approximately 10^{-13} J), which corresponds to the amplitude of the MW electric field at the fourth antinode $E_{MW} \approx 10$ V/cm [19]. Oscillations of σ_{xx} are clearly observed above 0.7 T for $n_s = 2.8 \times 10^7$ cm^{-2}. Oscillation amplitude strongly increases with lowering electron density.

It is important that we completely exclude the possibility that the observed magnetooscillations originate from MW-induced electron transitions to the first excited surface subband [10, 11] or from transitions between higher excited subbands [20]. For the first case, transitions appear only when the MW frequency matches the inter-subband transition frequency $\omega_{2,1}$, which can be Stark-tuned by the electric (pressing) field applied normal to the surface. For electrons on liquid ^{4}He, this frequency is measured to be about 126 GHz at zero pressing field [21], and it increases with the pressing field. Thus, in our experiment, the frequency of MW is at least 38 GHz lower than the transition frequency $\omega_{2,1}$. This is overwhelmingly larger than the corresponding transition linewidth which is about 10 MHz at $T = 0.56$ K [22]. Moreover, the excitation of inter-subband resonance requires the vertical component of $\mathbf{E}_{MW}$, which is significantly reduced in the present setup due to employment of the TEM. Finally, we find that the appearance of magnetoconductivity oscillations is independent of the applied pressing field in the range at least 40 V/cm. This corresponds to the upshift of inter-subband transition frequencies by at least 30 GHz.

Figure 3 shows σ_{xx} versus ω/ω_c for $n_s = 1.7 \times 10^7$ cm^{-2}, $T = 0.56$ K and several different values of the incident power P_{in}. This graph proves that the observed oscillations are periodic in ω/ω_c and exhibit an asymmetric shape in the vicinity of integer ω/ω_c, similar to MIRO in GaAs/AlGaAs heterostructures (though data reported in Ref. 2 differ from data of Refs.1, 3, 4). At $P_{in} = 100\ \mu$W, the amplitude of oscillations is about 50% of the "dark" value of σ_{xx}.

The main oscillatory features shown in Figs. 2 and 3 are in qualitative accordance with the displacement model of MIRO applied to SEs on liquid helium [15], where the shape of oscillations is described by the derivative of a Gaussian function $\partial G\left(\omega - m\omega_c\right)/\partial\omega$ broadened due to interactions. When varying temperature between 0.35 K and 0.56 K, the amplitude of oscillations approximately remains constant in spite of strong changes in the electron-ripplon interaction ($U_q^2 \propto T$), which also agrees with the displacement model. Still, at maximum power used here, the magnitude of oscillations given by

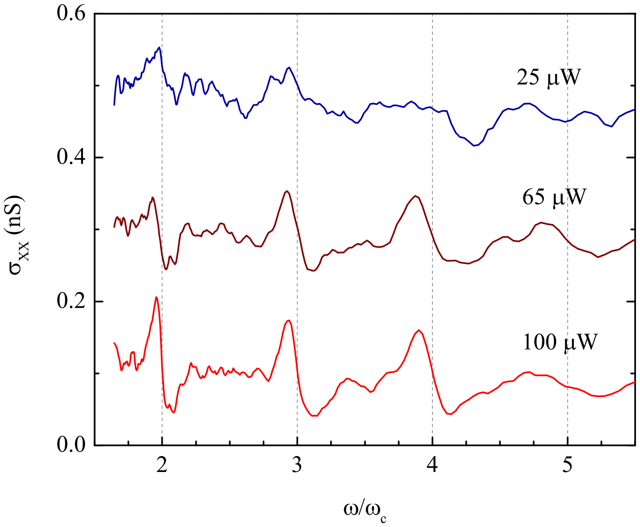

FIG. 3: (color online) σ_{xx} versus ω/ω_c for $T = 0.56$ K, $n_s = 1.7 \times 10^7$ cm^{-2} and different values of the incident MW power P_{in}. For clarity, curves for $P_{in} = 25$ (dark blue) and 65 μW (brown) are upshifted by 0.4 and 0.2 nS respectively.

the theory can reach the observed values only if Coulomb interaction is disregarded. In this case, the width of oscillatory features defined by the averaged broadening $\Gamma_{0,m} = \sqrt{\left(\Gamma_0^2 + \Gamma_m^2\right)/2}$ is substantially smaller than in our data. Coulomb forces induce additional broadening of the Gaussian $\Gamma_{0,m}^* = \sqrt{\Gamma_{0,m}^2 + x_q\Gamma_C^2}$, where $\Gamma_C = \sqrt{2}E_f^{(0)} l_B$, $x_q = q^2 l_B^2/2$ and $E_f^{(0)} \simeq 3\sqrt{T} n_s^{3/4}$ is the typical fluctuational electric field acting on an electron [23, 24]. This makes the width of oscillatory features comparable to the experimental data. Naturally, the amplitude of oscillations diminishes and becomes an order of magnitude smaller than that shown in Fig. 2.

Oscillatory features confined near $\omega/\omega_c = 2$, 3, and 4 are well separated; between them σ_{xx} irregularly varies near "dark" values with an amplitude practically independent of MW power. This distinguishes oscillations observed here from MIRO in heterostructures, and indicates the importance of Landau quantization for their origin. At low n_s, the signal-to-noise ratio decreases due to a weak current, therefore measurements at lower densities which might result in observation of ZRS become very challenging. Hear we didn't study photo-conductivity response near $\omega/\omega_c = 1$ because under the CR condition already very low incident MW power causes strong overheating of SEs which affects σ_{xx}.

Unfortunately, other theoretical mechanisms of MIRO discussed in the literature (reviewed in Ref. 5) are developed for a degenerate gas of noninteracting electrons and cannot be used for comparing with our data. Extensions of these models applicable to a nondegenerate system of strongly interacting electrons requires complicated studies which cannot be presented in this work. In addition to the displacement model, here we briefly discuss only the extension of the inelastic model, because it is also associated with photon-assisted scattering.

The SCBA theory [25] applied to electrons on liquid helium interacting with ripplons defines the effective collision frequency [15]

$$\nu = \frac{T}{\pi^2 n_s M l_B^4} \sum_n r_{n,n} \int d\varepsilon \left[-\frac{\partial f(\varepsilon)}{\partial \varepsilon} \right] g_n^2(\varepsilon), \qquad (1)$$

where $f(\varepsilon)$ is the electron distribution function, $-g_n(\varepsilon)$ is the imaginary part of the single-electron Green's function which represents the Landau level density of states,

$$r_{n,n'} = \frac{1}{\hbar T} \sum_{\mathbf{q}} U_q^2 x_q J_{n,n'}^2(x_q), \qquad (2)$$

$J_{n,n'}^2(x_q)$ is determined by $\left| \left(e^{-i\mathbf{q}\cdot\mathbf{r}}\right)_{n,X,n',X'} \right|^2 = \delta_{X,X'+l_B^2 q_y} J_{n,n'}^2(x_q)$. In Eq.(1) the overlapping of different levels is neglected. For low levels, $g_n(\varepsilon)$ is well described by a Gaussian function [26].

The MW field affects the electron distribution function $f(\varepsilon) \simeq f_T(\varepsilon) + \tilde{f}(\varepsilon)$, where $f_T(\varepsilon) \propto e^{-\varepsilon/T}$, and $\tilde{f}(\varepsilon)$ is a correction caused by photon-assisted scattering. If the fraction of electrons excited to the level $n' = m(B) \equiv \mathrm{round}(\omega/\omega_c)$ is small, a simple rate equation yields

$$\tilde{f}(\varepsilon) = \lambda\chi \frac{4 f_T(\varepsilon - \hbar\omega)\, g_0(\varepsilon - \hbar\omega)\, r_{0,m} T}{\hbar \nu_m^{(2r)}}. \qquad (3)$$

Here $\lambda = e^2 E_{MW}^2 / 4 M_e^2 \omega^4 l_B^2$, while χ depends only on ω/ω_c; (it approaches 2 if $\omega/\omega_c \to \infty$). The inelastic relaxation rate $\nu_m^{(2r)}$ is caused by emission of pairs of short wavelength ripplons [27] with $2\omega_{r,q} \simeq m\omega_c$. The two-ripplon interaction is important only for iter-level relaxation, while a quasi-uniform fluctuational field E_f cannot lead to iter-level transitions if $\Gamma_C \ll \hbar\omega_c$.

Eq. (3) determines $\tilde{f}$ only for ε near ε_m. For noninteracting SEs, the shape of the "imprint" of the ground level density $g_0(\varepsilon - \hbar\omega)$ is preserved because transitions to higher levels occurs with $\hbar\omega_{r,q} \ll \Gamma_n$. The sharp maximum of $g_0(\varepsilon - \hbar\omega)$ is the origin of sign-changing terms in Eq. (1). The new integrand factor $g_0(\varepsilon - \hbar\omega)\, g_n^2(\varepsilon)$ selects levels nearest to the condition $\varepsilon_n - \varepsilon_0 = \hbar\omega$. A fast drift velocity $\mathbf{u}_f$ of the electron orbit center in the fluctuational field $\mathbf{E}_f$ leads to an inelastic correction in the energy conservation $\hbar\mathbf{q}\cdot\mathbf{u}_f \simeq eE_f(X' - X)$, and averaging over $\mathbf{E}_f$ results in additional broadening ($x_q^{1/2}\Gamma_C$) of the maximum of $\tilde{f}(\varepsilon)$. Since backward transitions caused by two-ripplon emission are strongly inelastic ($2\omega_{r,q} \sim m\omega_c \gg \Gamma$), we assume that at the ground level $\tilde{f}(\varepsilon)$ is smoothed out and can be neglected for low excitations.

In the inelastic model, the shape of σ_{xx} variations is also described by the derivative of Gaussian functions $\partial G(\omega - m\omega_c)/\partial\omega$ broadened (slightly differently) due to interactions. As compared to the displacement model, these variations has an additional large factor $\sqrt{\pi} r_{m,m} T / \nu_m^{(2r)} \sqrt{\Gamma_m^2 + x_q \Gamma_C^2}$. The result of calculations performed for $n_s = 1.7 \times 10^7$ cm^{-2}, $T = 0.56$ K, and $E_{MW} = 2$ V/cm is shown in Fig. 2 by the dashed line. For high B, oscillatory features are confined near $\omega/\omega_c = m$ which agrees with our data. At low B, the broadening of terms with different m increases and they start overlapping. Then, the minima of σ_{xx} approach the condition $\omega/\omega_c(B) \to m + 1/4$. This also agrees with positions of minima at large m shown in Fig. 3.

It should be noted that the theoretical curve shown in Fig. 2 is obtained for a smaller amplitude of the MW field $E_{MW} = 2$ V/cm than that estimated for our data. If we include two-ripplon relaxation over intermediate levels ($n < m$), approximately the same amplitude of oscillatory features is found at $E_{MW} = 3$ V/cm. At $E_{MW} \sim 10$ V/cm, the assumption of small excitation used above fails, and power saturation becomes important. One can conclude that power saturation should restrict the amplitude of oscillatory features especially those confined near small m. This explains rather weak power dependence of the amplitude of oscillations which follows from Fig. 3. Also, one cannot exclude that small nonuniformity of $\mathbf{E}_f$ can give an additional contribution to the inelastic relaxation rate reducing $\tilde{f}$. Still, experimental estimation of the inelastic relaxation rate of SEs heated by the CR [28] agrees with the result of the theory of two-ripplon relaxation used in Eq. (3).

In summary, for the first time in the nondegenerate 2D system of strongly interacting electrons on liquid helium we observed MW-induced dc magnetoconductivity oscillations governed by the ratio ω/ω_c which are similar to those discovered in heterostructures. This proves the universality of the effect of MIRO, and potentially could help with identification of its origin. A new feature observed for high magnetic fields is that oscillatory variations are strongly confined near $\omega/\omega_c = 2, 3$, and 4; positions of minima are not fixed to "magic" numbers $m + 1/4$ which is in contrast with data obtained for GaAs/AlGaAs [2]. We report also a new many-electron effect: the amplitude of oscillations observed increases strongly with lowering electron density, which is in agreement with the many-electron treatment of photon-assisted scattering. Preliminary analysis shows that the observation can be explained by an oscillatory correction to the electron distribution function caused by photon-assisted scattering (inelastic model) affected by strong internal forces.

This work was supported by an internal grant from Okinawa Institute of Science and Technology (OIST) Graduate University. We thank S. A. Vasiliev for fruitfull discussions and V. P. Dvornichenko for technical support.

---

[*] E-mail: denis@oist.jp

[1] M.A. Zudov, R.R. Du, J. A. Simmons, and J.L. Reno, Phys. Rev. B **64**, 201311 (2001).

[2] R. Mani, J.H. Smet, K. von Klitzing, V. Narayanamurti, W.B. Johnson, and V. Umansky, Nature **420**, 646 (2002).

[3] M.A. Zudov, R.R. Du, L.N. Pfeiffer, and K. W. West, Phys. Rev. Lett. **90**, 046807 (2003).

[4] C.L. Yang, M.A. Zudov, T.A. Knuuttila, R.R. Du, L.N. Pfeiffer, and K.W. West Phys. Rev. Lett. **91**, 096803 (2003).

[5] I.A. Dmitriev, A.D. Mirlin, D.G. Polyakov, and M.A. Zudov, Rev. Mod. Phys. **84**, 1709 (2012).

[6] A.C. Durst, S. Sachdev, N. Read, and S.M. Girvin, Phys. Rev. Lett. **91**, 086803 (2003).

[7] V. Ryzhii and R. Suris, J. Phys.: Cond. Matt. 15, 6855 (2003).

[8] I.A. Dmitriev, A.D. Mirlin, and D.G. Polyakov, Phys. Rev. Lett. **91**, 226802 (2003).

[9] I.A. Dmitriev, M.G. Vavilov, I.L. Aleiner, A.D. Mirlin, and D.G. Polyakov, Phys. Rev. B **71**, 115316 (2005).

[10] D. Konstantinov and K. Kono, Phys. Rev. Lett. **103**, 266808 (2009).

[11] D. Konstantinov and K. Kono, Phys. Rev. Lett. **105**, 226801 (2010).

[12] Yu.P. Monarkha, Fiz. Nizk. Temp. **37**, 108 (2011) [Low Temp. Phys. **37**, 90 (2011)]; Yu.P. Monarkha, Fiz. Nizk. Temp. **37**, 829 (2011) [Low Temp. Phys. **37**, 655 (2011)].

[13] Yu.P. Monarkha, Fiz. Nizk. Temp. **38**, 579 (2012) [Low Temp. Phys. **38**, 451 (2012)].

[14] D. Konstantinov, Yu.P. Monarkha, and K. Kono, Phys. Rev. Lett. **111**, 266802 (2013).

[15] Yu.P. Monarkha, Fiz. Nizk. Temp. **40**, 623 (2014) [Low Temp. Phys. 40 , 482 (2014)].

[16] T. Peltonen, E. Tjukanof, J. Jarvinen, and S. A. Vasiliev, in *Proceedings of 3^{rd} ESA Workshop on Millimeter Wave Technology and Applications: Circuits, Systems, and Measurement Techniques, Espoo, 2003*, edited by J. Mallat, A. Raisanen, and J. Tuovinen (MilliLab, Espoo, Finland 2003).

[17] W.T. Sommer and D.J. Tanner, Phys. Rev. Lett. **27**, 1345 (1971).

[18] Yu.P. Monarkha and K. Kono, *Two-Dimensional Coulomb Liquids and Solids* (Springer-Verlag, Berlin, 2004).

[19] H. Kogelnik and T. Li, Proceedings of the IEEE **54**, 1312 (1966).

[20] D. Konstantinov and K. Kono, J. Low Temp. Phys. **158**, 324 (2010).

[21] C.C. Grimes and T.R. Brown, Phys. Rev. Lett. **32**, 280 (1974).

[22] E. Collin, W. Bailey, P. Fozooni, P.G. Frayne, P. Glasson, K. Harrabi, M.J. Lea, and G.Papageorgiou, Phys. Rev. Lett. **89**, 245301 (2002).

[23] M.I. Dykman and L.S. Khazan, Zh. Eksp. Teor. Fiz. **77**, 1488 (1979) [Sov. Phys. JETP **50**, 747 (1979)].

[24] C. Fang-Yen, M.I. Dykman, and M.J. Lea, Phys. Rev. B **55**, 16272 (1997).

[25] T. Ando and Y. Uemura, J. Phys. Soc. Jpn. **36**, 959 (1974).

[26] R.R. Gerhardts, Surf. Sci. **58**, 227 (1976).

[27] Yu.P. Monarkha, S.S. Sokolov, A.V. Smorodin, and N. Studart, Fiz. Nizk. Temp. **36**, 711 (2010) [Low Temp. Phys. **36**, 565 (2010)].

[28] V.S. Edel'man, Usp. Fiz. Nauk **130**, 675 (1980) [Sov. Phys. Usp. **23**, 227 (1980)].